Article

Antioxidant Capacity of Two Novel Bioactive Fe(III)-Cyclophane Complexes

Alex J. Salazar-Medina [1], Rocío Sugich-Miranda [1,2], Eli Teran-Cabanillas [2], Jesús Hernández [2], Gustavo A. González-Aguilar [2], Enrique Rudiño-Piñera [3], Rogerio R. Sotelo-Mundo [1,2,]* and Enrique F. Velázquez-Contreras [1,]*

[1] Departamento de Investigación en Polímeros y Materiales (DIPM), Universidad de Sonora, Calle Rosales y Blvd, Luis Encinas s/n, Col. Centro, PO Box 130. Hermosillo Sonora 83000, Mexico
[2] Centro de Investigación en Alimentación y Desarrollo (CIAD), A.C. Carretera a Ejido La Victoria Km 0.6, PO Box 1735, Hermosillo Sonora 83304, Mexico
[3] Departamento de Medicina Molecular y Bioprocesos, Instituto de Biotecnología, Universidad Nacional Autónoma de México (IBT-UNAM) Av. Universidad #2001, Col. Chamilpa, Cuernavaca, Morelos 62250, Mexico

* Authors to whom correspondence should be addressed; E-Mails: rrs@ciad.mx (R.R.S.-M.); evlzqz@guaymas.uson.mx (E.F.V.-C.); Tel./Fax: +52-662-259-2161 (E.F.V.-C.).

Abstract: The cyclophanes 2,9,25,32-tetraoxo-4,7,27,30-tetrakis(carboxymethyl)-1,4,7,10, 24,27,30,33-octaaza-17,40-dioxa[10.1.10.1]paracyclophane (**PO**) and 2,9,25,32-tetraoxo-4,7,27,30-tetrakis(carboxymethyl)-1,4,7,10,24,27,30,33-octaaza[10.1.10.1]paracyclophane (**PC**) were coordinated with iron to form cationic binuclear Fe(III) **Fe₂PO** and **Fe₂PC** complexes, respectively. Their antioxidant capacity, superoxide dismutase and peroxidase mimetic activity, as well as their toxicity toward peripheral blood mononuclear cells (PBMCs) were evaluated. Both **Fe₂PO** and **Fe₂PC** are interesting biomimetics with antioxidant capacity similar to that of ascorbic acid that prevent mortality in cultured PBMCs, with the potential to have bioactive and protective functions in disease animal models.

Keywords: cyclophane; macrocycle; iron; biomimetic; antioxidant

1. Introduction

Reactive oxygen species (ROS) are toxic molecules implicated in several human pathological processes including tissue injury, inflammation, ageing, cancer, cardiovascular, pulmonary and neurodegenerative diseases [1]. Aside from many enzymatic and chemical antioxidants, several synthetic metal complexes have shown activity as biomimetic antioxidants [2]. Transition metal complexes [e.g., complexes of Mn(II), Mn(III), Cu(II) and Fe(III)] have important antioxidant properties [1], due to their ability to change their oxidation state and their chemical interactions with a wide number of negatively charged ions, radicals and molecules. These characteristics have prompted the design and development of metal-based drugs with promising pharmacological application which might offer unique therapeutic opportunities [3].

The first line of defense against ROS in cellular systems is superoxide dismutase (SOD), that catalyzes the conversion of $O_2^{\bullet-}$ to H_2O_2 and O_2 [4]. Some macrocyclic complexes have been proposed as SOD mimetics, mainly because of their high thermal stability and flexible ligand arrangement that allows redox processes based on their metal centers [5]. The action of SOD produces H_2O_2 by the $O_2^{\bullet-}$ dismutation, a much less reactive molecule compared to $O_2^{\bullet-}$, but still toxic to the cell. H_2O_2 in the presence of transition metals, it is rapidly converted via the Fenton reaction to the hydroxyl radical ($^{\bullet}OH$). The $^{\bullet}OH$ is widely accepted to be the most damaging and cytotoxic ROS produced by cells. Two enzymes participate in the removal of H_2O_2 from the cellular environment, peroxidases (POx) and catalases (CAT), converting the H_2O_2 into water molecules and diatomic oxygen [6]. For these reasons we examined the use of Fe(III) ions coordinated to cyclophane ligands generating a new binuclear Fe(III)-cyclophane group of complexes, which could represent a new class of antioxidants. The study of these molecules will provide a deeper insight into the understanding of complexes that could mimic some enzymes related to ROS contention mechanisms.

2. Results and Discussion

2.1. Synthesis of the *PO* and *PC* Iron Complexes

The purified chelating cyclophanes 2,9,25,32-tetraoxo-4,7,27,30-tetrakis (carboxymethyl)-1,4,7,10, 24,27,30,33-octaaza-17,40-dioxa[10.1.10.1] paracyclophane (**PO**) and 2,9,25,32-tetraoxo-4,7,27,30-tetrakis(carboxymethyl)-1,4,7,10,24,27,30,33-octaaza[10.1.10.1] paracyclophane (**PC**), were synthesized as previously reported [7]. Both molecules were derived from ethylenediaminetetraacetic acid (EDTA) and provided with amino, amide and carboxymethyl pendant donor groups. Their purity was confirmed by melting/decomposition point (MDP) and NMR studies (see Experimental section below). Reactions between $FeCl_3 \cdot 6H_2O$ (at pH ~ 3) and **PO** and **PC** (both at pH ≤ 7), gave binuclear Fe(III) complexes $[Fe_2L]^{2+}$, labeled **Fe₂PO** and **Fe₂PC**, respectively (Figure 1). We propose that **PO** and **PC** metal chelates have a structure in which each Fe atom is coordinated by two carboxylate oxygens, two amine nitrogens and two amide oxygen atoms, with a feasible water molecule axial coordinated in aqueous solutions, on the basis of the well-known ferric EDTA complexes [8] and the coordination mode found in the X-ray crystal structure of a related cyclophane (3,10,21,28-tetraoxo-5,8,23,26-tetrakis(carboxymethyl)-2,5,8,11,20,23,26,29-octaaza[12.12] paracyclophane) bound to zinc [9]. **Fe₂PO**

was soluble in aqueous solutions in a pH range from 4.2 to 10.0, while **Fe₂PC** was soluble in aqueous solutions in a pH range from 5.2 to 10.0.

Figure 1. Chemical structures proposed of **Fe₂PO** and **Fe₂PC** cyclophane iron (III) complexes.

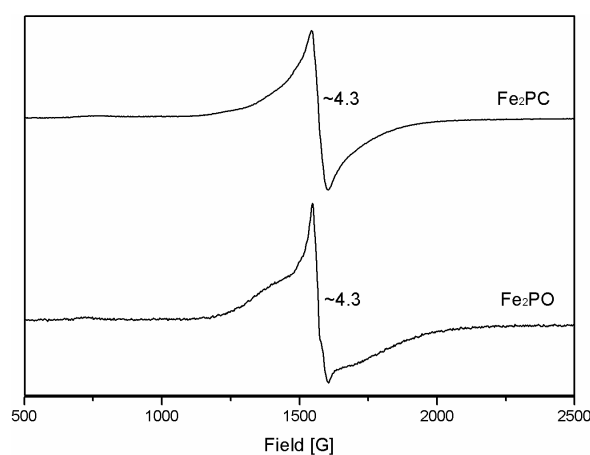X= -O- for Fe₂PO
X= -CH₂- for Fe₂PC
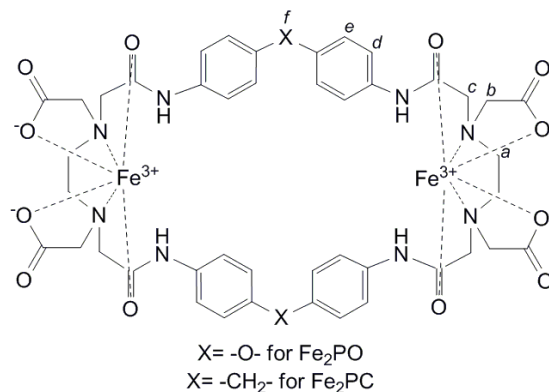
2.2. Mass Spectrometry

To confirm the formation of the metal complexes, the mass spectra of methanol-water solutions of **Fe₂PO** and **Fe₂PC** were obtained. **Fe₂PO** showed a major peak assigned to $[Fe_2^{3+}L^{4-}]^{2+}$ specie at $m/z = 510$ with an abundance of 100%. Another peak that supports the formation of the binuclear Fe(III) complex correspond to $[Fe_2^{3+}L^{4-}Cl^{2-}]$ at $m/z = 1,092$ with an abundance of 6%. For **Fe₂PC** a major peak assigned to $[Fe_2^{3+}L^{4-}]^{2+}$ specie was observed at $m/z = 508$ with an abundance of 100%. Molecular ion peaks corresponding to mononuclear species $[Fe^{3+}L^{-4}]^-$ were not detected for **Fe₂PO** or **Fe₂PC**.

2.3. Electron Paramagnetic Resonance (EPR)

The X-band EPR spectra observed for **Fe₂PO** and **Fe₂PC** in 60% aqueous methanol solutions at 6 K are shown in Figure 2. The spectra exhibit an intense peak at g ~ 4.3 in the region of 1,500 G, typical of high-spin ($S = 5/2$) iron(III) complexes with low symmetry, as well as commonly found in a variety of solid state materials, chelates and metallo proteins [10,11].

Figure 2. g values of the X-band EPR spectra for **Fe₂PO** and **Fe₂PC**. Experimental conditions: methanol/water (6:4) matrix, temperature 6 K, microwave frequency 9.338 GHz, modulation 1 G.

2.4. Infrared Spectroscopy

The coordination mode for **Fe₂PO** and **Fe₂PC** complexes was analyzed by IR spectroscopy by comparison of absorption bands of the non-coordinated ligand *vs.* the metal complex (Figure 3). The stretching carbonyl bands gave shifts from 1,684 cm^{-1} (**PO**) to 1,620 cm^{-1} (**Fe₂PO**) and 1,674 cm^{-1} (**PC**) to 1,624 cm^{-1} (**Fe₂PC**). We also observed a broad OH band at the 3,200–3,600 cm^{-1} region. The changes in the position of the absorption bands of Fe-bound and unbound cyclophanes provide us an indicative of the formation of the metal complex and its preferred coordination sites in the ligand structures, as well as the observed for Fe(III)-EDTA complexes [8].

Figure 3. IR spectra for KBr pellets of (**a**) **PO** and **Fe₂PO** (solid and dotted line respectively); and (**b**) **PC** and **Fe₂PC** (solid and dotted line respectively).
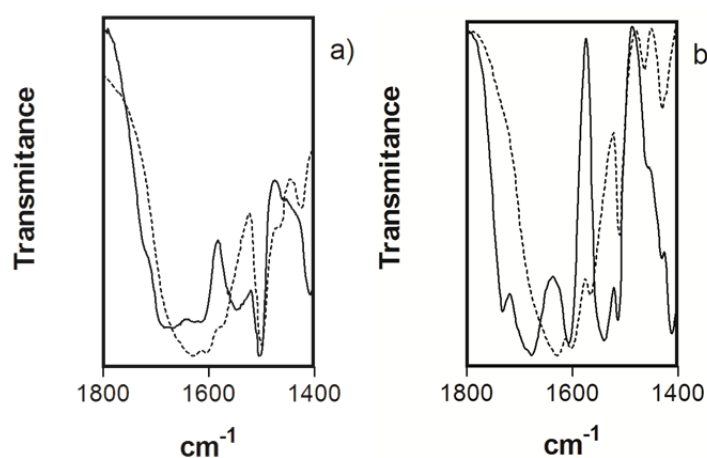
2.5. Electronic Absorption Spectra

The electronic spectra for **Fe₂PO** solution were pH dependent, as shown in Figure 4(a). In a pH range of 6.0 to 10.0 the spectra show two bands with a λ_{max} of 350 nm ($\varepsilon_{pH7.0}$ = 11,830 M^{-1}cm^{-1}) and 475 nm ($\varepsilon_{pH7.0}$ = 4,680 M^{-1}cm^{-1}), assigned to a ligand-to-metal charge transferences (LMCT) [12]. With an increase of the pH, the molar absorptivity also increases, and the λ_{max} of each band was slightly displaced to a major wavelengths. Above pH ~ 10, the molar absorptivity of the LMCT bands decreases due to the precipitation of the complex in the working solution. The data obtained in the UV-Vis experiment were analyzed through the program Excel® Worksheets for Spectrometry [13] and we determined the presence of different protonation state species of the **Fe₂PO** complex [Figure 5(a)], where the non-deprotonated species $Fe_2L(H_2O)_2$ reaches its maximum concentration at pH 6.0 and then start to decrease. Over this pH, the **Fe₂PO** complex solution becomes into a dark red colored solution and the mono deprotonated species $Fe_2L(H_2O)(OH)$ and bi deprotonated species $Fe_2L(OH)_2$ appears, to finally shift into a yellow colored suspension (precipitate complex) at pH 11.0. These spectrophotometric observations are consistent with those corresponding to the complex Fe(III)-EDTA [14].

Figure 4. Solution electronic spectra of (**a**) **Fe₂PO** and (**b**) **Fe₂PC** at different pH values. White and black circles spectra corresponded to unbound cyclophane and Fe(III) respectively, both at pH ~ 7, as a controls.
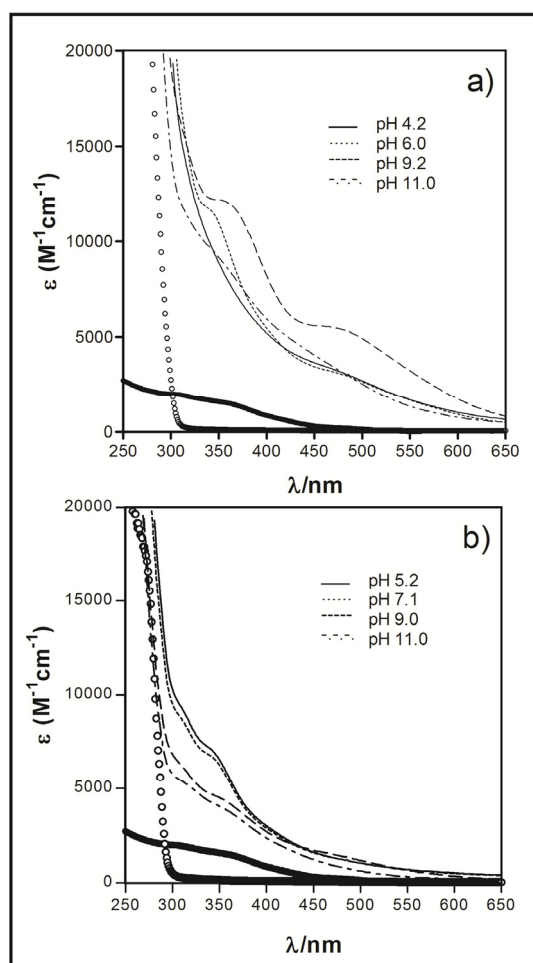
The electronic spectra of Fe₂PC also present two LMCT bands, the first one at 307 nm ($\varepsilon_{pH7.0}$ = 8,710 $M^{-1}cm^{-1}$), and the second band at 334 nm ($\varepsilon_{pH7.0}$ = 6,270 $M^{-1}cm^{-1}$). In this case, the intensity of the two bands decreases with the augmentation of the pH [Figure 4(b)]. The same method of analysis was used to establish the presence of different protonation state species of **Fe₂PO**, and it was utilized with the UV-Vis data spectra of **Fe₂PO** complex [Figure 5(b)]. The non-deprotonated species $Fe_2L(H_2O)_2$ moves its maximum concentration percentage from pH 6.0 for **Fe₂PO** to pH 6.5 for **Fe₂PC** and then starts to decrease. Over pH ≈ 8.0 the deprotonated species appears, $Fe_2L(H_2O)(OH)$ and $Fe_2L(OH)_2$, and the complex solution becomes a dark red colored solution, to finally shift into a yellow colored suspension due to the formation of the precipitate complex over pH 11.0, as well as that observed to **Fe₂PO**.

As a consequence of the pH dependence mentioned above, a mixture of the species $Fe_2L(H_2O)_2$ and $Fe_2L(H_2O)(OH)$ of **Fe₂PO** as well as **Fe₂PC**, was present in each experiment described below (Figure 6).

Figure 5. Correlation between the species distribution and the absorption spectra of **Fe₂PO** at top and **Fe₂PC** at bottom. (% = Percentage of species distribution in solution).
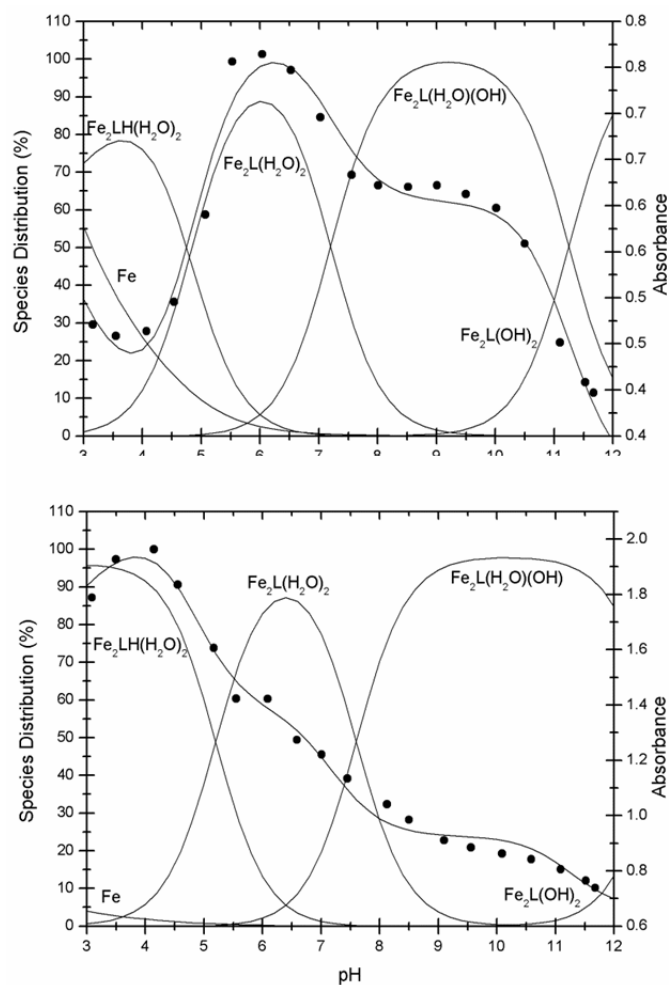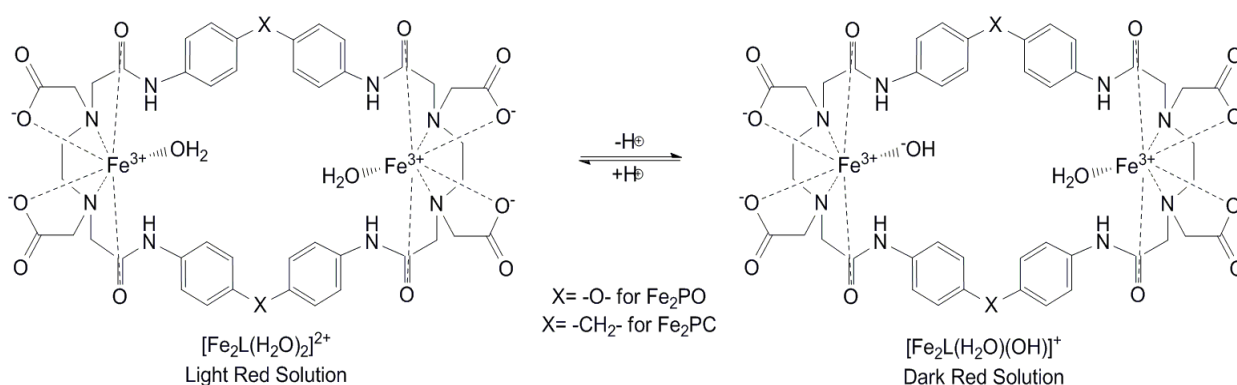

Figure 6. Changes in protonation state of the aqueous solutions of **Fe₂PO** and **Fe₂PC** complexes in dependence of pH.


The differences between the substituent groups X = -O- for **Fe₂PO** and X = -CH₂- for **Fe₂PC** (Figure 1), provide the Fe(III) complexes with distinct properties, even with the no participation of the substituent groups in the coordination sphere with iron. X = -O- allows a major flexibility to **Fe₂PO** against the **Fe₂PC**, because the more rigidity property of X = -CH₂- and this characteristic is responsible of the differences in the UV-Vis spectra behavior between **Fe₂PO** and **Fe₂PC**. Even

though the two iron atoms coordinate to the same groups in **PO** and **PC** ligands, a higher tension was expected to **Fe₂PC** complex to maintain the coordination. In addition, **Fe₂PO** has shown major solubility in aqueous solution, letting us to study it at lower pHs than Fe₂PC do. In the species distribution diagram we can see the non-protonated and protonates species of **Fe₂PO** and **Fe₂PC** appear at different pH values, behavior attributable to the structural rigidity in each metal complex.

2.6. Antioxidant Capacity Assay

The characterization of antioxidant capacity is of great importance because the multiple biological and medical applications of such synthetic molecules. The **Fe₂PO** had more antioxidant capacity (0.0690 g eq Trolox mol^{-1}) than **Fe₂PC** (0.0443 g eq Trolox mol^{-1}), both within the range of the antioxidant capacity presented by ascorbic acid at the same molar concentration (0.0755 g eq Trolox mol^{-1}) (Figure 7). The behavior of the Fe(III) complexes was similar to the observed for the Cu(II) complexes reported by Sugich-Miranda and co-workers [5]. The difference between **Fe₂PO** and **Fe₂PC** antioxidant capacity could be due to differences in conformational flexibility of **Fe₂PC**, resulting in a less favorable interaction with the ABTS$^{•+}$ radicals in solution causing a lower antioxidant capacity. The antioxidant capacity of iron (FeCl₃) was undetectable in the TEAC assay.

Figure 7. Antioxidant capacity of **Fe₂PO** and **Fe₂PC** complexes by the TEAC assay. Ascorbic acid and a solution of Fe(III) were used as a controls. Bars represent the standard error of the mean (±SEM) of triplicate experiments. Ferric chloride had no detectable antioxidant capacity and was not plotted.
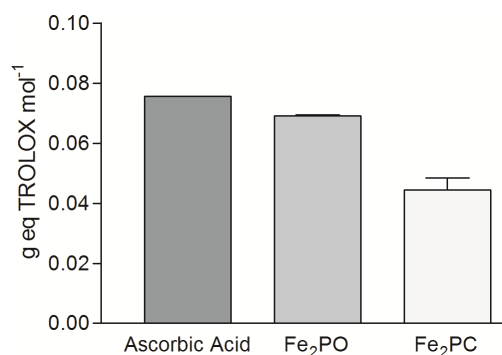
2.7. Superoxide Dismutase-Like Activity

The SOD-like activity was measured by inhibition of the oxidation of nitrobluetetrazolium (NBT) induced by the presence of the $O_2^{•-}$ radical generated by the xanthine and xanthine oxidase enzymatic system. We tested bovine SOD as the main scavenger of $O_2^{•-}$ radical, producing 89.40% of NBT oxidation inhibition with a 60 μM concentration of the enzyme. Under the same conditions the NBT oxidation inhibition of **Fe₂PO** was 39.53% and for **Fe₂PC** was 41.97% (Figure 8). The values obtained of both metal complexes, reaches over a 44% of NBT oxidation inhibition generated by bovine SOD.

Figure 8. SOD-like activities of **Fe₂PO** and **Fe₂PC** complexes as inhibitors of the NBT oxidation. Bars represent the standard error of the mean (±SEM) of triplicate values.
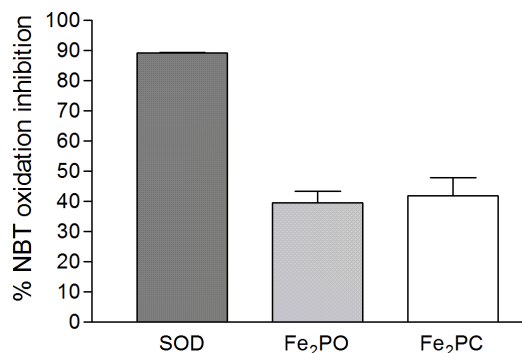
2.8. Peroxidase-Like Activity

In order to investigate the bioactive capacity as a POx mimetic, the POx-like activity of **Fe₂PO** and **Fe₂PC** complexes was determined using the Amplex$^{®}$ Red Hydrogen Peroxide/Peroxidase Assay Kit. The results observed were 0.13 and 0.29 nm of Amplex$^{®}$ Red oxidized min^{-1} mg^{-1} complex for **Fe₂PO** and **Fe₂PC**, respectively. Both **Fe₂PO** and **Fe₂PC** complexes kept the POx-like activity for about 48 h, as observed with a continuous oxidation of the Amplex$^{®}$ Red reagent in presence of H_2O_2 (Figure 9). This prolonged capacity of **Fe₂PO** and Fe₂PC to act as a POx mimetic towards H_2O_2 is desirable in a chemical with pharmacological properties. For example, the HRPO, as the main peroxidase tested in this assay, was only active *in vitro* for 30 min, compared to the 48 h of the cyclophane biomimetic complexes. Likewise, for a hemoglobin recombinant protein of the plant *Arabidopsis thaliana*, another class of POx mimetic, a rapid inactivation was observed after 30 s, although the great initial specific activity [15]. Therefore, the study of the possible mechanisms of these mimetic chemicals will give useful knowledge for the medical and pharmacological area.

Figure 9. Peroxidase-like activity of ● FeCl₃, ■ PO, ▲ PC, ▼ Fe₂PO and ♦ Fe₂PC. Bars represent the standard error of the mean (±SEM) of triplicate values.
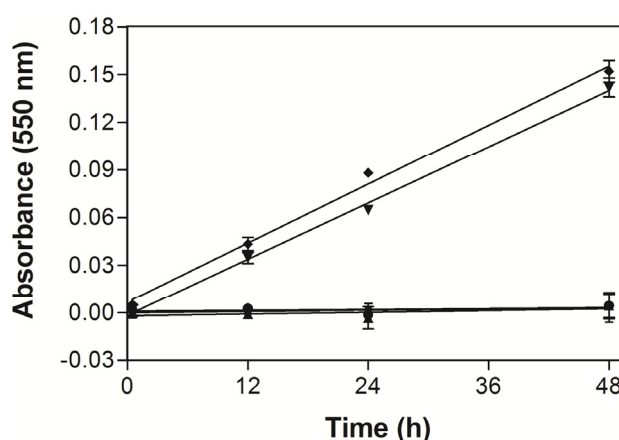

2.9. Cellular Assay

To evaluate the bio-protective effect of Fe(III)-cyclophane complexes, different concentrations of **Fe₂PO** and **Fe₂PC** (30, 60 and 120 μM) were incubated with PBMCs in the presence of xanthine plus

xanthine oxidase to generate reduced species of oxygen and induce cell damage. The percentage of mortality was evaluated by trypan blue dye exclusion assay. Figure 10(a) shows that **Fe₂PO** reduced mortality percentage in all the concentrations probed from 10.6% in control untreated cells to 5.06% with the highest concentration (120 μM) tested, after 24 h of culture. A similar trend was for **Fe₂PC** [Figure 10(b)], reducing the mortality from 10.7% in control untreated cells to 4.70% with the highest concentration tested, after 24 h of culture. We previously evaluated the toxicity after 24 h culture of the Fe(III)-cyclophane complexes and the highest percentages of mortality for **Fe₂PO** and **Fe₂PC** was 0.9% and 0.5%, respectively. These results are similar to those previously reported by our group [5], where we found no toxic but a protective effect of the **Cu₂PO** and **Cu₂PC** in PBMCs by reducing mortality in 6% compared to control untreated cells. These results indicate that both cyclophane-Fe(III) complexes were not cytotoxic during the first 24 h of culture, even when high doses were used. Therefore, these molecules could be considered as potential candidates for further antioxidant studies using animal models and cancer cell lines in order to probe its possible beneficial effects. Over 24 h of culture the cell mortality increases because lacking of nutrients in the culture medium.

Figure 10. Cellular protection of (**a**) **Fe₂PO** and (**b**) **Fe₂PC** in PBMCs with induced damage by ROS. The line marked as blank corresponds to PBMCs in RPMI medium with no treatment. Data comes from a representative experiment. Points represent the standard error of the mean (±SEM) of triplicate values.
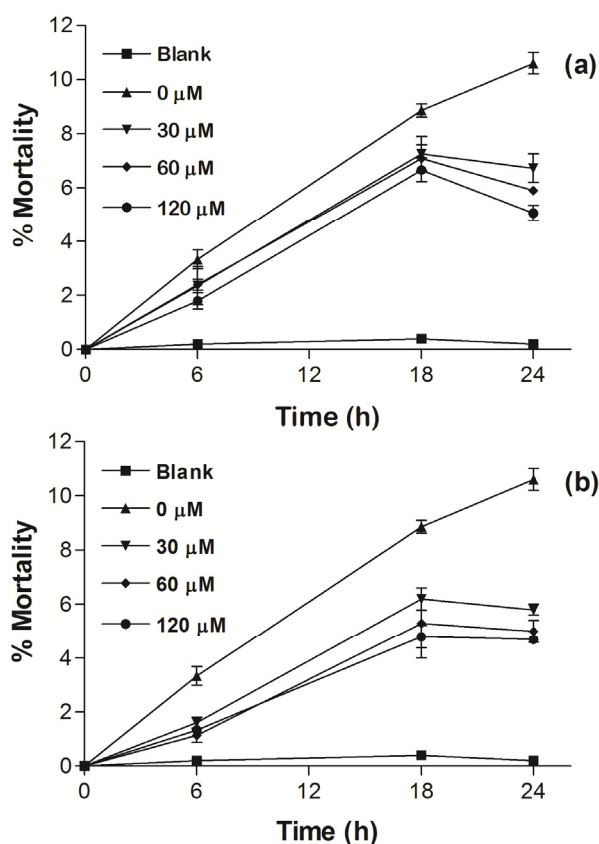
3. Experimental

3.1. Syntheses of Cyclophanes and Iron Complexes

PO was synthesized by adding bis(4-aminophenyl) ether (Aldrich, 1.5 g) in dimethylformamide (DMF, 70 mL) dropwise to ethylenediamine tetraacetic (EDTA) dianhydride (Aldrich, 2.0 g) in DMF (200 mL) under a nitrogen atmosphere. The light yellow solution obtained was concentrated and mixed with water, and a pale brown solid was obtained. This crude cyclophane was converted to the lithium salt, and recrystallized twice from hot water. Acidification (pH ~ 3) of the purified lithium salt gave **PO** in the acid form as a colorless solid. Yield: 15%. MDP: 262.0 °C. The absence of impurities such as oligomers was confirmed by ^{1}H-NMR (D$_2$O/Na$_2$CO$_3$, pD = 9.5, 400 MHz, DSS): δ_H = 2.86 (8H, s, Hb), 3.29 (8H, s, Ha), 3.43 (8H, s, Hc), 6.85 (8H, d, He), 7.18 (8H, d, Hd).

PC was synthesized by essentially the same method as for PO by the use of the diamine bis (4-aminophenyl)methane (Aldrich). The crude product was converted to the lithium salt, which was recrystallized from 50% ethanol. When an aqueous solution of the purified lithium salt was acidified with diluted HCl to pH ~ 3, **PC** in the acid form was obtained as a colorless solid. The product was washed with water. Yield: 12%. MDP: 256.0 °C. ^{1}H-NMR (D$_2$O, pD = 10.4; 400 MHz; DSS): δ_H = 2.81 (8H, s, Hb); 3.28 (8H, s, Ha), 3.38 (8H, s, Hc), 3.78 (4H, s, Hf), 6.98 (8H, d, He), 7.12 (8H, d, Hd).

To obtain the iron (III) complexes, each host molecule (either **PO** or **PC**) was dissolved in water and solubilized by adding a minimum amount of solid Na$_2$CO$_3$. This solution was added to an aqueous solution containing a slight excess of FeCl$_3$·6H$_2$O, the binuclear iron complex precipitated in a quantitative yield. The melting decomposition point (MDP) was obtained in a Mel-Temp II equipment (Laboratory Devices). The electrospray ionization (ESI) mass spectra were obtained by the use of a JEOL HX 110A spectrometer for sample solutions of methanol-water mixture.

Fe$_2$PO. MDP: 301.7 °C. MS (ESI): *m/z* (for (C$_{44}$H$_{44}$Fe$_2$N$_8$O$_{14}$)$^{2+}$) = 510 (100) ([Fe$_2$$^{3+}$L^{4-}]$^{2+}$);

Fe$_2$PC. MDP: 283.8 °C. MS (ESI): *m/z* (for (C$_{46}$H$_{48}$Fe$_2$N$_8$O$_{12}$)$^{2+}$) = 508 (100) ([Fe$_2$$^{3+}$L^{4-}]$^{2+}$).

3.2. Spectroscopic Measurements

The EPR spectra of the binuclear Fe(III) complexes were obtained on an X-band continuous wave Elexsys E500 (Bruker) EPR spectrometer, for 60% aqueous methanol solutions. The final concentration of each complex was approximately 1 mM. Infrared spectra were recorded on a Perkin Elmer Spectrum GX FT-IR system, in the range 4,000–400 cm^{-1}. The samples were prepared as KBr pellets. The solution electronic spectra were obtained by the use of an Agilent 8453A UV-VIS diode array spectrometer. The pH of the samples solutions was adjusted by adding the necessary amount of NaOH solution. The species distributions were determined using the data obtained in the UV-Vis analysis varying the pH, with the program Excel® Worksheets for Spectrometry [13].

3.3. Antioxidant Capacity Assay

The Trolox equivalent antioxidant capacity (TEAC) assay is based on determination of Trolox-equivalents, which is a water-soluble analog of vitamin E. Trolox (6-hydroxy-2,5,7,8-tetramethylchroman-2carboxylic acid) was purchased from Aldrich (Milwaukee, WI, USA). ABTS (2,2-azino-bis(3-

ethylbenzthiazoline-6-sulfonic acid), potassium persulfate ($K_2S_2O_8$) and ascorbic acid (vitamin C) were obtained from Sigma Chemical Co. (St. Louis, MO, USA). All other reagents were analytical grade or better. **Fe₂PO** and **Fe₂PC** complexes were evaluated at 30 and 60 µM concentrations using a modified TEAC method to determine their antioxidant activity. The TEAC method measures the antioxidant capacity to scavenging the blue-green ABTS$^{•+}$ radical cation versus the scavenging capacity of Trolox. The radical cation ABTS$^{•+}$ was obtained by mixing 5 mL of 7 mM ABTS solution and 88 µL of a 140 mM $K_2S_2O_8$ solution. One milliliter of the ABTS$^{•+}$ was dissolved in 88 mL of PBS. In a quartz cell, the reaction contained 245 µL of an ABTS$^{•+}$ and 5 µL of each test sample or dilutions of the Trolox standards. The absorbance was read within 80 min after the initial mixing. Calculations were made correlating the scavenging capacity of Trolox *versus* each sample. The antioxidant capacity was expressed as grams equivalent Trolox per mol of test sample.

3.4. Superoxide Dismutase-Like Activity

SOD activity was determined according to Beyer and Fridovich [16] with slight modifications as follows: the stock solution consisted of 2 mM xanthine (50 µL), 0.3% Triton X-100 solution (50 µL), 1.2 mM nitrobluetetrazolium (NBT, 50 µL), 0.1 mM phosphate buffer solution (770 µL, pH 7.8) and xanthine oxidase enzyme (600 mU mL^{-1}, 20 µL) to start the reaction; 1 mM (60 µL) of each sample, **Fe₂PO** or **Fe₂PC** (for a final concentration of 60 µM) were added to the quartz cell by triplicate. Then, the quartz cell was mounted into a UV-visible spectrophotometer (Varian), and the absorbance was measured (at 540 nm for 5 min) as absorbance increment due to NBT formation per unit of time. Assays were performed at room temperature (25 °C). We reported the inhibition percentage of tetrazolium formazan formation, under the conditions describe above.

3.5. Peroxidase-Like Activity

POx activity was determined using the Amplex® Red Hydrogen Peroxide/Peroxidase Assay Kit. The assay consisted in placing into individual wells of a microplate 50 µL of working solution prepared as follows: 10 mM Amplex® Red (10-acetyl-3,7-dihydroxyphenoxazine) reagent stock solution (50 µL), 20 mM H_2O_2 solution (500 µL) and 1X Reaction Buffer (4.45 mL) and **Fe₂PO** or **Fe₂PC** (50 µL) were added with a final concentration of 0.1 mM. The POx activity was determined spectrophotometrically monitoring the oxidation of the Amplex® Red reagent to Resourfin in the presence of H_2O_2 and a POx or POx mimetic, using a microplate reader at 550 nm after 0.5, 12, 24 and 48 h of incubation.

3.6. Cellular Assay

PBMCs were isolated from heparinized blood obtained from human healthy donors by a density gradient centrifugation using Ficoll-Hypaque. Isolated PBMCs (5×10^5 cells per well) were resuspended in RPMI-1640 medium containing 10% heat-inactivated fetal calf serum, 50 mM 2-mercapoethanol, 100 U mL^{-1} amphotericin band seeded onto 96-well tissue culture plates for stimulation with phytohemagglutinin (PHA, 5 µg mL^{-1}) in the presence of enzymatic system, xanthine plus xanthine oxidase (XO), as an enzymatic generator of reactive oxygen species, *i.e.*, superoxide, hydrogen

peroxide and hydroxyl radicals [16] (8 mM of xanthine and 23 mU mL^{-1} XO), and a different concentrations of **Fe₂PO** and **Fe₂PC** (0, 30, 60 and 120 µM). Cells were incubated 6, 18 and 24 h at 37 °C in 5% CO_2. Cell viability was evaluated by trypan blue dye exclusion assay.

4. Conclusions

Two novel Fe(III)-cyclophanes have shown bioactive properties as antioxidants, reducing the synthetic ABTS$^{•+}$ radical, within the range observed for ascorbic acid, which was used as the reference antioxidant. Reported results for similar Cu(II) complexes [5] demonstrated the biomimetic potential of these metallic cyclophane derivatives [7]. Aside of their antioxidant capacity comparable to phenolic acids, flavonoids and vitamins C and E [17] is the lack of need for negative interactions with cells. For that matter, a bioassay using PBMC cells injured with ROS was done to test their antioxidant capacity *in vivo*. In fact, both **Fe₂PO** and **Fe₂PC** were able to scavenge the superoxide produced by xanthine and xanthine oxidase, leading to an increased cellular survival.

The differences in biomimetic activity between **Fe₂PO** and **Fe₂PC** could be due to structural differences between the cyclophanes. The action of iron-cyclophanes against the superoxide radical was similar in the SOD assay, while when a stable radical (ABTS) was used to test antioxidant capacity, **Fe₂PO** was better than **Fe₂PC**. It is known that **PC** is more rigid compared to **PO**, and since ABTS is a large molecule with a mass over 500 Da, we postulate that steric effects arise at the interaction with the synthetic antioxidant. Considering that these molecules could remove superoxide radical and led to molecular water that not affect cells, they appear to be very interesting molecules for further studies to evaluate their antioxidant and bioactive properties in animal models and cancer cell lines.

References

1. Fernandes, A.S.; Gaspar, J.; Cabral, M.F.; Caneiras, C.; Guedes, R.; Rueff, J.; Castro, M.; Costa, J.; Oliveira, N.G. Macrocyclic copper (II) complexes: Superoxide scavenging activity, structural studies and cytotoxicity evaluation. *J. Inorg. Biochem.* **2007**, *101*, 849–858.
2. Jakab, I.N.; Lrincz, O.; Jancsó, A.; Gajda, T.; Gyurcsik, B. Approaching the minimal metal ion binding peptide for structural and functional metalloenzyme mimicking. *Dalton Trans.* **2008**, *2008*, 6987–6995.
3. Rafique, S.; Idrees, M.; Nasim, A.; Akbar, H.; Athar, A. Transition metal complexes as potential therapeutic agents. *Biotechnol. Mol. Biol. Rev.* **2010**, *5*, 38–45.
4. Muscoli, C.; Cuzzocrea, S.; Riley, D.P.; Zweier, J.L.; Thiemermann, C.; Wang, Z.Q.; Salvemini, D. On the selectivity of superoxide dismutase mimetics and its importance in pharmacological studies. *Br. J. Pharmacol.* **2003**, *140*, 445–460.

5. Sugich-Miranda, R.; Sotelo-Mundo, R.R.; Silva-Campa, E.; Hernández, J.; Gonzalez-Aguilar, G.A.; Velazquez-Contreras, E.F. Antioxidant capacity of binuclear Cu (II)-Cyclophanes, insights from two synthetic bioactive molecules. *J. Biochem. Mol. Toxicol.* **2010**, *24*, 379–383.

6. Rodriguez, C.; Mayo, J.C.; Sainz, R.M.; Antolin, I.; Herrera, F.; Martin, V.; Reiter, R.J. Regulation of antioxidant enzymes: A significant role for melatonin. *J. Pineal Res.* **2004**, *36*, 1–9.

7. Inoue, M.B.; Velazquez, E.F.; Medrano, F.; Ochoa, K.L.; Galvez, J.; Inoue, M.; Fernando, Q. Binuclear copper (II) chelates of amide-based cyclophanes. *Inorg. Chem.* **1998**, *37*, 4070–4075.

8. Kanamori, K.; Dohniwa, H.; Ukita, N.; Kanesaka, I.; Kawai, K. The raman spectral study on the solution structure of iron (III)-EDTA complexes. *Bull. Chem. Soc. Jpn.* **1990**, *63*, 1447–1454.

9. Inoue, M.B.; Medrano, F.; Inoue, M.; Raitsimring, A.; Fernando, Q. A New Chelating Cyclophane and Its Complexation with Ni^{2+}, Cu^{2+}, and Zn^{2+}: Spectroscopic Properties and Allosterism via Ring Contraction. *Inorg. Chem.* **1997**, *36*, 2335–2340.

10. Bou-Abdallah, F.; Chasteen, N.D. Spin concentration measurements of high-spin (g' = 4.3) rhombic iron (III) ions in biological samples: Theory and application. *J. Biol. Inorg. Chem.* **2008**, *13*, 15–24.

11. Namuswe, F.; Hayashi, T.; Jiang, Y.; Kasper, G.D.; Sarjeant, A.A.N.; Moënne-Loccoz, P.; Goldberg, D.P. Influence of the Nitrogen Donors on Nonheme Iron Models of Superoxide Reductase: High-Spin FeIII-OOR Complexes. *J. Am. Chem. Soc.* **2009**, *132*, 157–167.

12. Dhungana, S.; Heggemann, S.; Gebhardt, P.; Möllmann, U.; Crumbliss, A.L. Fe (III) coordination properties of a new saccharide-based exocyclic trihydroxamate analogue of ferrichrome. *Inorg. Chem.* **2003**, *42*, 42–50.

13. Inoue, M. Excel® Worksheets for Spectrometry 2012. Universidad de Sonora, Hermosillo, Sonora, México, 2012.

14. Bull, C.; McClune, G.J.; Fee, J.A. The mechanism of iron EDTA catalyzed superoxide dismutation. *J. Am. Chem. Soc.* **1983**, *105*, 5290–5300.

15. Sakamoto, A.; Sakurao, S.; Fukunaga, K.; Matsubara, T.; Ueda-Hashimoto, M.; Tsukamoto, S.; Takahashi, M.; Morikawa, H. Three distinct *Arabidopsis* hemoglobins exhibit peroxidase-like activity and differentially mediate nitrite-dependent protein nitration. *FEBS Lett.* **2004**, *572*, 27–32.

16. Beyer, W.F.; Fridovich, I. Assaying for superoxide dismutase activity: Some large consequences of minor changes in conditions. *Anal. Biochem.* **1987**, *161*, 559–566.

17. Aispuro-Hernandez, E.; Garcia-Orozco, K.D.; Muhlia-Almazan, A. Shrimp thioredoxin is a potent antioxidant protein. *Comp. Biochem. Physiol. C Toxicol. Pharmacol.* **2008**, *148*, 94–99.

Sample Availability: Samples of the compounds **PO**, **PC**, **Fe₂PO** and **Fe₂PC** are available from the authors.